Unique Adsorption Properties and Potential Energy Profiles of Microporous Pillared Clays

M. S. A. Baksh and R. T. Yang
Dept. of Chemical Engineering, State University of New York, Buffalo, NY 14260

The adsorption isotherms of O_2, N_2, CH_4, CO_2, SO_2, and NO on five pillared clays (Zr, Al, Cr, Fe, and Ti-PILCs) are measured. The equilibrium selectivity of CH_4/N_2 on Al-PILC is greater than 5.0, which exceeds all known sorbents by a large margin. In addition, high SO_2/CO_2 equilibrium selectivities are observed on these pillared clays. The sorption characteristics of these pillared clays (PILCs) exhibit characteristic trends that are better understood with the aid of the potential energy profiles. A new semi-empirical approach is presented for the calculations of the potential energy profiles of PILCs. This approach requires the adsorption isotherms and an isotherm equation that accounts for the structural heterogeneity of the adsorbents. A comparison of the energy profiles obtained using the semi-empirical approach with the corresponding results obtained via the Kirkwood-Muller formalism, where only dispersion forces are taken into account, provides a measure of the importance of the electrostatic forces in the sorption characteristics of these PILCs. Sizable differences are observed for the potential energy profiles, indicating that the electrostatic forces are not negligible, and can significantly enhance the adsorption potential, resulting in large increases in the amounts adsorbed on these PILCs.

Introduction

Pillared interlayered clays (PILCs) are two-dimensional zeolite-like materials prepared by exchanging the charge-compensating cations between the clay layers with large inorganic hydroxycations, which are polymeric or hydroxy metal cations formed by hydrolysis of metal oxides or salts (Baes and Mesmer, 1976). Upon calcination, the resulting materials contain metal oxide pillars which prop open the clay sheets and thereby expose the internal surfaces of the clay layers. Much interests and research have been directed toward the synthesis of Al-PILC (Brindley and Sempels, 1977; Vaughan et al., 1979, 1981; Lahav et al., 1978; Shabtai et al., 1984; Pinnavaia et al., 1984; Occelli, 1984; Sterte, 1991; Suzuki et al., 1988; Occelli and Tindwa, 1983; Burch, 1988; Figueras, 1988), Zr-PILC (Vaughan et al., 1979, 1981; Yamanaka and Brindley, 1979; Figueras et al., 1989; Burch and Warburton, 1986; Bartley and Burch, 1985; Yang and Baksh, 1991), Cr-PILC (Tzou and Pinnavaia, 1988; Carrado et al., 1986; Hopkins et al., 1984; Vaughan, 1987; Shabtai and Lahari, 1980; Pinnavaia et al., 1985), Fe-PILC (Yamanaka and Hattori, 1988; Yamanaka et al., 1984; Burch and Warburton, 1987; Lee et al., 1989; Pinnavaia and Tzou, 1987; Warburton, 1988; Rightor et al., 1991), and Ti-PILC (Sterte, 1986). In addition, several experimental parameters such as the concentration of the metal ion, the basicity or degree of hydrolysis (given as $r = OH/M$), temperature of preparation, time and temperature of aging, type of counterion, and the method of preparation can affect the degree of polymerization of the hydroxy-oligomeric cations in aqueous solution (Baksh, 1991) and consequently the physicochemical properties of the pillared clays.

The adsorption isotherms of gases on microporous adsorbents provide valuable information in the determination of molecular forces between the gas molecules and the adsorbent atoms. Unfortunately, only limited adsorption isotherms of various adsorbates on pillared clays exist in the literature. The short list of "sorbent" studies is limited to a small number of adsorption isotherm measurements (Occelli et al., 1985; Bandoz et al., 1989; Tzou and Pinnavaia, 1988; Yamanaka and Hattori, 1988) and diffusivities studies (Occelli et al., 1985;

Correspondence concerning this article should be addressed to R. T. Yang.

Tzou and Pinnavaia, 1988; Sahimi et al., 1988). Therefore, to further elucidate the sorption characteristics of pillared clays (a new class of adsorbents) and evaluate it suitability as adsorbents, additional isotherm measurements are needed. As an alternative to the measurements of adsorption isotherms, computer simulations can be conducted to predict the adsorption isotherms. For example, Rowley et al. (1976), Peterson et al. (1988), Woods et al. (1988), June et al. (1990), Metropolis et al. (1953), Kiselev and Du (1981), Nicholson and Parsonage (1982), Soto and Myers (1981), Karavias and Myers (1991), Adams (1975), Razmus and Hall (1991), and Stroud et al. (1976) have used computer simulations (such as Monte Carlo, molecular dynamics, mean field density functional) for predicting the adsorption isotherms and thermodynamic properties of various adsorbates on molecular sieves. The results from such simulations are then used in determining important parameters which are characteristic of a given gas-solid system.

In contrast to sophisticated computer simulations, simple models (Baksh and Yang, 1991; Saito and Foley, 1991; Horvath and Kawazoe, 1983) exist and are useful for calculating the potential energy profiles and pore size distributions of molecular sieves (such as zeolites and carbons). Everett and Powl (1976) have calculated the potential energy profiles for atoms adsorbed in slit-like pores and showed the enhancement of the depth of the potential energy well over that for adsorption on a flat surface. Using a slit model, Horvath and Kawazoe (1983) provided a method for the calculation of effective pore size distribution from the adsorption isotherms in molecular sieve carbon. Analogous methods for cylindrical and spherical pores are given by Saito and Foley (1991) and Baksh and Yang (1991), respectively.

In this study, the adsorption properties of five pillared clays (Zr, Al, Cr, Fe, and Ti PILCs) are examined. The adsorbates selected are N_2, O_2, CH_4, CO_2, NO, and SO_2, since separations of mixtures of these gases are of commercial importance. For example, air (N_2/O_2) separation (Yang, 1987), NO_x/SO_2 (Kikkinides and Yang, 1991), CO_2/CH_4 (Kapoor and Yang, 1989), and N_2/CH_4 (Baksh et al., 1990; Ackley and Yang, 1990) separations. In addition, a new semi-empirical approach is introduced to aid in the calculations of the potential energy profiles in pillared clays. These energy profiles are quite useful in explaining the sorption properties of pillared clays.

Since the mean pore sizes of pillared clays, obtained from probe molecules sorption data, are smaller than the free interlayer spacings (Baksh, 1991; Baksh et al., 1992), the pores in pillared clays consist of narrow and tall paths, limited by interpillar spacings. Although, the pore structures of pillared clays are quite complex, the slit-like geometry seems to be more realistic than the cylindrical (Saito and Foley, 1991), and spherical (Baksh and Yang, 1991) geometries. However, because a semi-empirical approach is used in calculating the energy profiles and the pore size distributions, we can use the slit-like, cylindrical or spherical pore models to represent the complicated pore structures of pillared clays. In this work, we used the slit-like model and the 10:4 parallel plate potential function (Everett and Powl, 1976) to illustrate the numerical scheme.

The first step requires the evaluation of the constants in the 10:4 model. This step requires the adsorption isotherms and parameters from the Jaroniec-Choma equation (Jaroniec and Choma, 1987). Once the constants in the 10:4 model are determined, the potential energy profiles are calculated readily for a selected adsorbate. As an alternative, the constants of the 10:4 model can be evaluated from physicochemical data of the gas/solid system and the utility of existing equations such as the Kirkwood-Muller equation (Baksh and Yang, 1991). Such an approach, however, depends heavily on accurate physicochemical data and neglects the importance of other intermolecular forces (for example, electrostatic) that can be quite significant, resulting in incorrect potential energy profiles. To establish the accuracy of the Kirkwood-Muller equation, the energy profiles obtained from the semi-empirical approach are compared, and the differences in the profiles are indicative of the importance of forces other than dispersion that are responsible for the observed macroscopic sorption properties of the various gas-solid systems.

Experimental Procedure

The composition of the pillared clays were determined using an inductively coupled argon plasma atomic emission spectrometer (ICAP-AES). The experimental details can be found elsewhere (Baksh, 1991; Liche et al., 1987). A Quantasorb Surface Area Analyzer (Quantachrome Corporation) was used for BET surface area measurements. Prior to each measurement, the sample was outgased at 200°C for 15 h. The N_2 isotherms (at 77 K) were also used for pore size distribution calculations.

Equilibrium adsorption isotherms were measured with the aid of a microbalance (Mettler TA 2000C Thermoanalyzer), which was connected to a gas flow system. The flow system and the experimental procedures were the same as those described elsewhere (Baksh et al., 1991). Stringent steps were taken in the design, calibration and operation of the TGA/flow system to minimize or eliminate the undesirable factors which often plague the measurements of adsorption isotherms: nonisothermal effect, buoyancy force, and traces of moisture. The carrier gas (helium) and the adsorptive gases were purified and dried by passing through presorbers before entering the balance. Samples of less than 50 mg were used in the measurements of adsorption isotherms.

Theory

Review of slit model

The slit-potential model of Everett and Powl (1976) can be used for adsorption in microporous pillared clays, since the pores in these materials are slit-like. Excellent reviews of these theories are offered by Baksh and Yang (1991), Saito and Foley (1991), and Suzuki (1990). Only a brief outline is given here to aid in forthcoming discussions. Everett and Powl (1976) showed that the potential energy of interaction, ϵ, between one adsorbate molecule and two parallel lattice planes whose nuclei are at a distance L apart, can be expressed via the Lennard-Jones potential as:

$$\epsilon = K\epsilon^* \left[-\left(\frac{\sigma}{r}\right)^4 + \left(\frac{\sigma}{r}\right)^{10} - \left(\frac{\sigma}{L-r}\right)^4 + \left(\frac{\sigma}{L-r}\right)^{10} \right] \quad (1)$$

where

$$\sigma = \left(\frac{2}{5}\right)^{1/6} d_o$$

$K=3.07$, d_o is the arithmetic mean of the diameters of the adsorbate and adsorbent, and r is the displacement of a molecule from the plane of surface nuclei (one plate).

In the case of more than one adsorbate molecule, the value of ϵ^* in Eq. 1 is:

$$\epsilon^* = \frac{3}{10}\left[\frac{N_a A_a + N_A A_A}{d_o^4}\right] \tag{2}$$

where the dispersion constants are given by the Kirkwood-Muller formalism as:

$$A_a = \frac{6mc^2\alpha_s\alpha_A}{\left(\frac{\alpha_s}{\chi_s}\right)+\left(\frac{\alpha_A}{\chi_A}\right)} \tag{3}$$

and

$$A_A = \frac{3}{2}(mc^2\alpha_A\chi_A) \tag{4}$$

By combining Eqs. 1 and 2, the potential function for the slit pore filled with adsorbate molecules can be written as:

$$\epsilon(r) = \frac{N_A A_A + N_a A_a}{2\sigma^4}\left[-\left(\frac{\sigma}{r}\right)^4 + \left(\frac{\sigma}{r}\right)^{10} - \left(\frac{\sigma}{L-r}\right)^4 + \left(\frac{\sigma}{L-r}\right)^{10}\right] \tag{5}$$

Horvath and Kawazoe (1983) used an energy balance and equated the free energy of adsorption to the net energy of interaction between the layers. Their result can be written as:

$$RT\ln(P/P_o) = N_{Av}\frac{\int_{d_o}^{L-d_o}\epsilon(r)dr}{\int_{d_o}^{L-d_o}dr} \tag{6}$$

Substituting Eq. 5 into Eq. 6, the Horvath and Kawazoe (1983) result for slit-like geometry becomes:

$$R_g T\ln(P/P_o) = N_{Av}\frac{N_A A_A + N_s A_s}{\sigma^4(L-2d_o)}\left[\frac{\sigma^4}{3(L-d_o)^3} - \frac{\sigma^{10}}{9(L-d_o)^9} - \frac{\sigma^4}{3d_o^3} + \frac{\sigma^{10}}{9d_o^9}\right] \tag{7}$$

Review of the J-C model

For a homogeneous or nearly-homogeneous microporous material, the Dubinin-Radushkevich (DR) adsorption equation is applicable:

$$a_{mi} = a_{mi}^o\exp[-B(RT/\beta)^2(\ln P_o/P)^2] = f(B) \tag{8}$$

where a_{mi} is the amount absorbed at pressure P, β is the affinity coefficient, usually based on $\beta=1$ for benzene as the reference sorbate, and B is the structural parameter which increases with an increase in pore sizes.

For materials with a distribution of pore sizes, the amount adsorbed is (Stoeckli, 1977; Dubinin and Stoeckli, 1980; Stoeckli, 1990):

$$a_{mi} = \int_0^\infty f(B)G(x)dx \tag{9}$$

where $G(x)$ is the pore size distribution function. For a Gamma-type distribution function,

$$G(x) = \frac{2(qc)^{n+1}}{\Gamma(n+1)}x^{2n+1}\exp(-qcx^2) \tag{10}$$

with a maximum at the point

$$x_m = \left[\frac{n+1/2}{qc}\right]^{1/2} \tag{11}$$

and a mean pore size ($\bar{x}$) given by:

$$\bar{x} = \phi_x\left[\frac{n+1}{qc}\right]^{1/2} \tag{12}$$

where

$$\phi_x = \frac{\Gamma(n+3/2)}{(n+1)^{1/2}\Gamma(n+1)} \tag{13}$$

Upon substituting the $G(x)$ function (Eq. 10) into Eq. 9, the following was obtained by Jaroniec and his coworkers (Jaroniec and Madey, 1987, 1988; Jaroniec et al., 1991) referred to as Jaroniec-Choma isotherm:

$$\frac{a_{mi}}{a_{mi}^o} = \left[\frac{q}{q+\left(\frac{RT}{\beta}\ln\frac{P_o}{P}\right)^2}\right]^{n+1} = \left[\frac{\bar{B}}{\bar{B}+\left(\frac{RT\sigma_B}{\beta}\ln\frac{P_o}{P}\right)^2}\right]^{(\bar{B}/\sigma_B)^2} \tag{14}$$

where

$$\bar{B} = \frac{n+1}{q}$$

and the standard deviation (σ_B):

$$\sigma_B = \frac{(n+1)^{1/2}}{q}$$

The procedures for calculating the micropore size distributions of pillared clays using Eq. 14 and probe molecules sorption data were described recently by Baksh et al. (1992).

Calculation of Energy Profiles

Equations for the constants in the 10:4 parallel plate model

As discussed by Walker (1966), it is difficult to decide which formulas to accept in calculating the dispersion constants, but the ones most frequently used are: Slater-Kirkwood, Kirkwood-Muller, London, Bardeen, and Margenau and Pollard. Derrah and Ruthven (1975) have used the Kirkwood-Muller, Slater-Kirkwood, and London formulae to estimate the potential energy functions of noble gases in 5A zeolite. After finding that various formulas produced quite different energy profiles, they concluded that for Kr and Xe, the Slater-Kirkwood formula agrees best with experimental data, while the London formula works best for Ar. In addition, the choice of which formula to use in evaluating dispersion constants could be dictated by the availability of experimental data for a given adsorbate/adsorbent system. For example, in using the London formula, the ionization potentials and the polarizabilities of the adsorbate and the adsorbent must be available. Thus, the selection of the formula could be reduced to the availability of experimental data, which could produce erroneous results for the potential energy profiles. In this study, the Kirkwood-Muller formalism (Eqs. 3 and 4) is selected for use in the 10:4 potential model. Other equations, however, could be used as well, since only dispersion forces are accounted for in these equations (Slater-Kirkwood, London, Kirkwood-Muller, and so on). The calculated energy profiles are then compared with the semi-empirical approach introduced in the next section. Any difference among the energy profiles obtained from the Kirkwood-Muller formalism and the semi-empirical model reflects the importance of intermolecular forces other than dispersion (such as electrostatic) in the sorption characteristics of PILCs.

Semi-empirical approach for calculating energy profiles

Some of the adsorption isotherms are measured at temperatures above the critical temperatures of the adsorbates, where the concept of saturation vapor pressures is meaningless. However, the Jaroniec-Choma (J-C) equation (Eq. 14), and the Horvath-Kawazoe (H-K) model (Eq. 7) require the relative sorption pressure (P/P_o). Therefore, above the critical temperatures of the adsorbates, one must estimate the vapor pressures at the adsorption temperatures. The reduced Kirchhoff equation (Yang, 1987; Reid and Sherwood, 1966) can be used for estimating the vapor pressures below and above the critical temperatures. The reduced Kirchhoff equation is:

$$P = P_c \exp\left[h\left(1 - \frac{1}{T_r}\right)\right] \tag{15}$$

where h is given by:

$$h = \frac{T_{nbp}}{T_c}\left[\frac{\ln P_c}{1 - \frac{T_{nbp}}{T_c}}\right] \tag{16}$$

Using the estimated vapor pressures, the adsorption isotherms can be translated (when necessary) as the amount adsorbed as a function of relative pressure. These data are then used in the J-C equation (Eq. 14) to obtain the parameters n, q and a^o_{mi}. The details of this step and the calculations of the pore size distributions can be found elsewhere (Baksh et al., 1992; Baksh and Yang, 1991; and references therein). Once the J-C pore size distribution for a given gas-solid system (such as N_2/Zr-PILC) is determined, a guess is made for the constant, $N_aA_a + N_AA_A$, in Eq. 7 (Horvath-Kawazoe model), and the pore size distribution calculated with the aid of the adsorption isotherm (Horvath and Kawazoe, 1983). The guess for the constant is assumed to be accurate when the pore size distributions obtained from the H-K model and the J-C model possess identical mean pore sizes. Once the constant ($N_aA_a + N_AA_A$) is determined, its value is substituted into Eq. 5 to calculate the potential energy profiles for that gas-solid system. Note that this approach does not involve the use of any equation that accounts only for dispersion forces (such as Kirkwood-Muller, London, and Slater-Kirkwood), and therefore the values obtained for the constants $N_aA_a + N_AA_A$ for different gas-solid systems will include all the intermolecular forces (such as dispersion, electrostatic, and induction), since these constants are determined empirically using the adsorption isotherms and the above procedures.

To illustrate the utility of the semi-empirical approach, the potential energy profiles of Al-PILC and Zr-PILC obtained using N_2 and CH_4 adsorption isotherms and the above procedures are included in this work. Also included are the potential energy profiles obtained using N_2 sorption isotherms at 77 K (Baksh et al., 1992) on five PILCs. The energy profiles are compared with the corresponding results obtained using the Kirkwood-Muller formalism to emphasize the errors that are present when forces other than dispersion are neglected. In addition, since the positions of point charges in the solid matrix (PILC) are not known accurately, the contributions of the electrostatic forces (such as electrostatic) become questionable, and only produced uncertainty in the calculated energy profiles, which can be easily removed using the semi-empirical approach.

Results and Discussions

Micropore size distributions of PILCs

The procedures, experimental data, and the values of the constants in Eq. 14 (J-C model) needed to determine the micropore size distributions of PILCs were discussed in a recent study (Baksh et al., 1992). The micropore size distributions of pillared clays (PILCs), obtained using the semi-empirical approach described above, and N_2 sorption data at 77 K are given in Figure 1A. The micropore size distributions determined from probe molecules (such as H_2O, N_2, C_6H_6, 1,3,5-trimethylbenzene, and perfluorotributylamine) sorption data (Baksh et al., 1992) are shown in Figure 1B. The theoretical and experimental micropore size distributions (Figures 1A and 1B, respectively) show that the pore sizes of the PILCs are in the order Cr < Zr < Al < Fe < Ti. The different pore sizes of PILCs influence tremendously the sorption characteristics due to the enhancement of sorption potential, which increases with decreasing pore sizes. To explain the sorption characteristics of pillared clays, it is necessary to show some preliminary results of enhancement of sorption potentials in slit-like pores (the pores in PILCs are approximately slit-like).

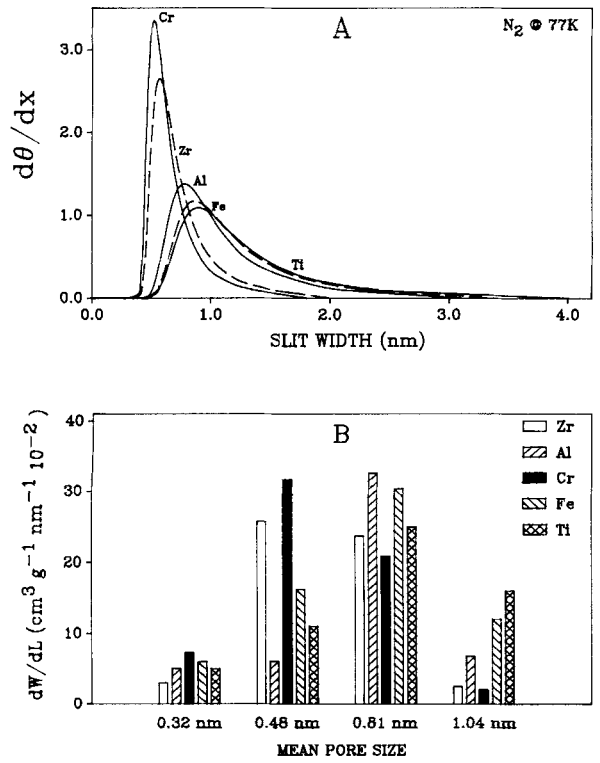

Figure 1. Micropore size distributions obtained from the Horvath-Kawazoe model (Eq. 7).

The values of $N_aA_a + N_AA_A$ (in Eq. 7) are determined from the semi-empirical model. The bar graphs (Figure 1B) give the micropore size distributions obtained from probe molecules sorption data.

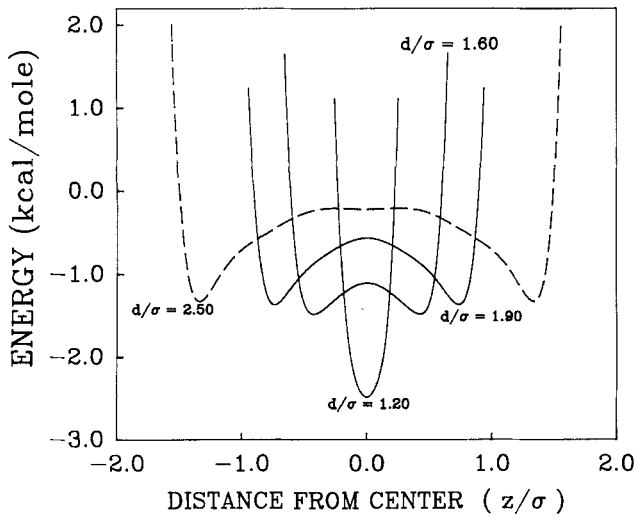

Figure 2. Potential energy profiles showing the enhancement of the adsorption potentials as a function of pore sizes (calculated from d/σ) and for an adsorbate placed at different positions (z/σ) between two parallel plates.

z = the distance from centerline, $z = 0$, corresponds to an adsorbate molecule placed equidistantly between the two plates. A value of 45 cal·nm^4/mol was used for $N_aA_a + A_AN_A$ in Eq. 5. This value was obtained from the semi-empirical model and the N_2 adsorption isotherm at 77 K on Zr-PILC.

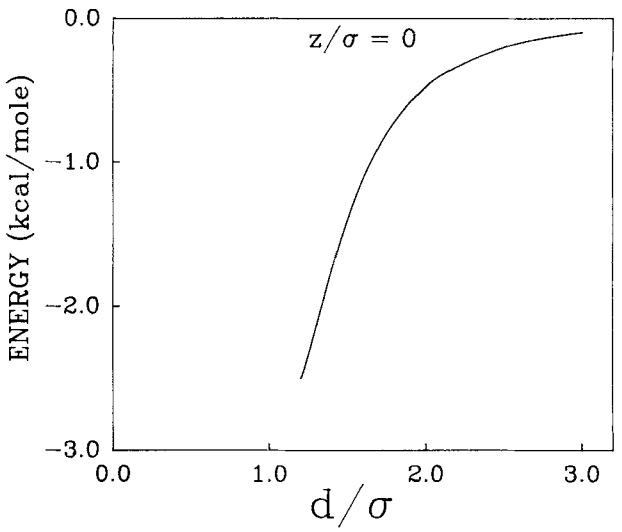

Figure 3. Potential energy at the centerline ($z/\sigma = 0$) as a function of pore sizes (calculated from d/σ).

A value of 45 cal·nm^4/mol was used for $N_aA_a + N_AA_A$ in Eq. 5.

Variations of sorption potentials with pore sizes

Figure 2 shows the potential energy, ϵ (see Eq. 5), as a function of z/σ for four different pore sizes (made dimensionless using $\sigma = 0.30$ nm). All the energy profiles of this figure are calculated using $N_aA_a + N_AA_A = 45$ cal·nm^4/mol (see Eq. 5). The value of 45 cal·nm^4/mol is determined from the N_2 isotherm at 77 K on Zr-PILC (Baksh et al., 1992) and the semi-empirical model described above. Note that the values of d correspond to one-half the pore sizes ($L = 2d$ in Eq. 5), r is the displacement of a molecule from a plane of surface nuclei (one plate), and $z = d - r$ is the distance of a molecule from the centerline: $z = 0$ corresponds to a molecule placed equidistantly between two parallel plates. For large d/σ, the potential energy curves exhibit two minima, whereas at small d/σ these minima coalesce to give a single minimum. Figure 3 shows the potential energy at the centerline ($z/\sigma = 0$) as a function of the pore sizes (d/σ). It is obvious from Figures 2 and 3 that for small pores (small d/σ), the potential energies decrease rapidly due to the overlapping of the attractive parts of the potential. Conversely, for large pore sizes (large d/σ), the potential energies at the centerline ($z = 0$) approach zero. It is important to note that only small variations in d/σ values can change significantly the adsorption potential in the slit-like micropores and consequently the sorption characteristics of the adsorbents.

Potential energy profiles of pillared clays

The potential energy profiles of five pillared clays (Zr, Al, Cr, Fe, and Ti PILCs) are displayed in Figure 4. These profiles are obtained using the semi-empirical model and the N_2 adsorption isotherms at 77 K (Baksh et al., 1992). The energy profiles are computed for d/σ values calculated from the mean pore sizes of the PILCs. Since Cr-PILC has the smallest pores, the enhancement in the sorption potential is the highest. However, as will be seen later, although Cr-PILC possesses the highest enhancement, the adsorption isotherm can reflect lower sorption capacity, since adsorbates with increasing diameters cannot penetrate the narrow pores. The location of the energy

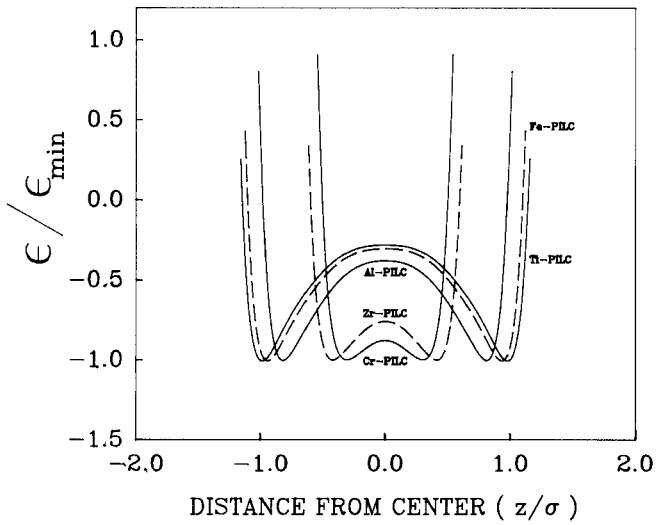

Figure 4. Potential energy profiles obtained from the semi-empirical model and the N_2 adsorption isotherms at 77 K.

minima are at larger z/σ values for increasing pore sizes. In addition, an adsorbate molecule (N_2 in this case) will experience repulsive force at smaller values of z/σ when the pore sizes decrease (smaller d/σ). The pore sizes of the PILCs are in the order Cr < Zr < Al < Fe < Ti.

The energy profiles obtained from the semi-empirical model and the adsorption isotherms of N_2 and CH_4 at 298 K are displayed in Figure 5. The physical properties of the adsorbates (N_2 and CH_4) used for estimating the vapor pressures via the reduced Kirchhoff correlation (see Eqs. 15 and 16) are given in Table 1. The physical properties of the other adsorbates used in this study are also tabulated for convenience. Since CH_4 has a larger kinetic diameter than N_2 (0.38 nm for CH_4 compared to 0.364 nm for N_2), N_2 can approach the plate closer than CH_4. Therefore, the potential energy well for N_2 for a given PILC is closer to the plate (larger z/σ). Also, the central maxima correspond to energy values that indicate the large molecule (CH_4) and experience greater enhancement in the sorption potential, that is, the central maximum for CH_4 is higher (more negative) than the central maximum of N_2 for a given PILC.

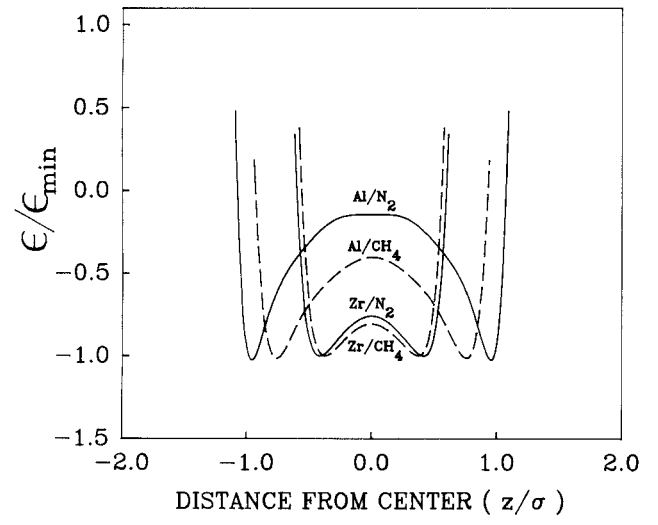

Figure 5. Potential energy profiles obtained from the semi-empirical model, N_2 and CH_4 adsorption isotherms at 298 K.

The reduced Kirchhoff equation (Eq. 15) was used for estimating vapor pressures above the critical temperatures of the adsorbates.

Table 1. Adsorbate's Critical Properties, Normal Boiling Points, h Values (Eq. 16), and Vapor Pressures at 298 K (Using Eqs. 15 and 16)

Adsorbate	T_{nbp} (K)	T_c (K)	P_c (atm)	T_r	h	P_o at 298 K (atm)
O_2	90.02	154.62	50.14	1.927	5.455	691.688
N_2	77.20	126.11	33.54	2.363	5.545	821.293
CH_4	112.00	190.40	45.44	1.565	5.452	325.279
CO_2	194.50	304.04	72.85	0.980	7.615	62.365
SO_2	263	430.50	77.90	0.692	6.839	3.712
NO	121.2	180.10	64.6	1.655	8.577	1925.137

Potential energy profiles of PILCs: semi-empirical model vs. Kirkwood-Muller (K-M) formalism

The utility of the Kirkwood-Muller formalism (Eqs. 3 and 4) requires physicochemical data on the adsorbate and adsorbent. The data used for calculating the potential energy profiles via the Kirkwood-Muller (K-M) formalism are tabulated in Table 2. The adsorbent density (N_a) of pillared clay can be estimated from the lattice constants of montmorillonite clay (Beutelspacher and Van Der Marel, 1968), by assuming that the density of adsorption sites on the clay surface equals to that on the pillar surface. This assumption is a reasonable first approximation, since the calculated N_a values obtained from the crystal structures of the oxides (pillars) do not deviate significantly from those of the clay surface. Such assumption was unavoidable, since no crystallographic information can be obtained on the pillars, because the pillars are so small (the pillars are contained within the clay layers) that data acquisition becomes impossible, due to the limiting capabilities of available instruments. The adsorbate (N_2) density is obtained from liquid N_2 density ($N_A = 6.17$ molecule/nm^2).

The amount of pillars can be determined using inductively coupled argon plasma atomic emission spectroscopy (Baksh et al., 1992; Baksh, 1991). The surface areas, amount of pillars, and the values of $N_aA_a + N_AA_A$ (see Eq. 5) needed for the calculation of the energy profiles using the Kirkwood-Muller formalism are given in Table 3. The values of $N_aA_a + N_AA_A$

Table 2. Physical Parameters Used for Calculating the Energy Profiles via Kirkwood-Muller Formalism (Eqs. 3 and 4)

Parameter	Adsorbent Oxide Ion	Adsorbate N_2
Diameter (nm)	0.276	0.364
Polarizability, α (cm^3/molecule)	2.5×10^{-24}	1.46×10^{-24}
Magnetic Susceptibility, χ (cm^3/molecule)	1.3×10^{-29}	2.0×10^{-29}
Density, N (molecules/nm^2)	31.52	6.17

Table 3. Physicochemical Properties of the Pillared Clays and N_2 Systems: Amount of Oxides (Pillars), Surface Areas, and the Values of the Constants ($N_aA_A + A_AN_A$) Obtained Using the Semi-empirical (SEM) Model*

Pillared Interlayered Clays (PILCs)				
Oxides (Pillars)	wt. %	BET m^2/g	LANG. m^2/g	$N_aA_a + N_AA_A$ (SEM) $cal \cdot nm^4/mol$
ZrO_2	17.65	322	494.45	45.0
Al_2O_3	10.46	295	470.56	62.0
Cr_2O_3	26.85	303	483.32	32.0
Fe_2O_3	27.20	217	325.50	68.0
TiO_2	30.17	258	351.00	70.0

*The value of $N_aA_a + N_AA_A$ obtained via the Kirkwood-Muller formalism (Eqs. 3 and 4) is 30.66 $cal \cdot nm^4/mol$.

determined from the semi-empirical model, and the N_2 adsorption data at 77 K (Baksh et al., 1992) on PILCs are included in the table. Note, that for Cr-PILC, the values of $N_aN_a + N_AA_A$ obtained from the Kirkwood-Muller (K-M) equation and the semi-empirical model are almost identical (30.66 vs. 32 $cal \cdot nm^4/mol$), whereas for the other PILCs, sizable differences are observed ($\leq 50\%$). Figures 6 and 7 show in detail the differences in the energy profiles obtained from the Kirkwood-Muller and the semi-empirical model. Since the Kirkwood-Muller formalism takes into account only dispersion forces, large deviations in the energy profiles are anticipated whenever forces

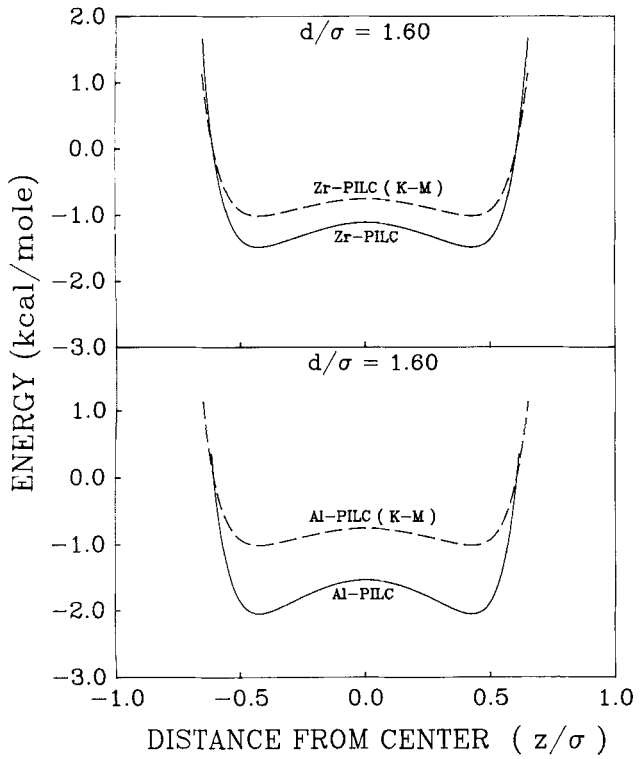

Figure 6. Potential energy profiles of Zr and Al-PILCs for a given pore size ($d/\sigma = 1.60$), using the semi-empirical model and the Kirkwood-Muller (K-M) formalism.

The N_2 adsorption data (Baksh et al., 1992) at 77 K on PILCs were used in the calculations.

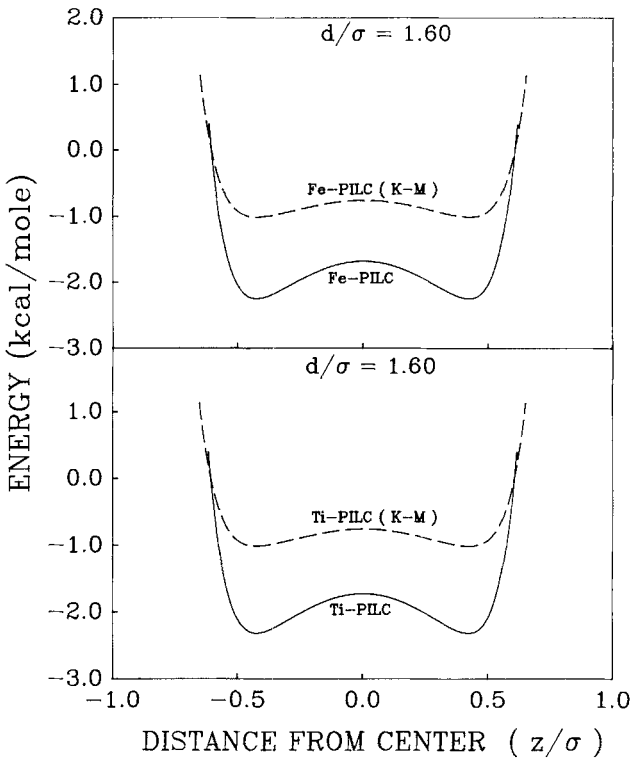

Figure 7. Potential energy profiles of Fe and Ti-PILCs for a given pore size ($d/\sigma = 1.60$), using the semi-empirical model and the Kirkwood-Muller formalism.

The N_2 adsorption data (Baksh et al., 1992) at 77 K were used in the calculations.

other than dispersion (such as electrostatic) are present. Therefore, the semi-empirical model can be useful for testing the validity of the Kirkwood-Muller formalism for various gas-solid systems.

Adsorption isotherms

The adsorption isotherms (at 298 K) of CH_4, N_2, CO_2, SO_2, O_2 and NO on five pillared clays are given in Figures 8–13. To facilitate the discussion, the kinetic diameters and related physical properties of the adsorbates are given in Table 4. Recall from Figure 1 that the pore sizes in pillared clays are in the order Cr < Zr < Al < Fe < Ti, and therefore the enhancement in the sorption potentials should follow, in accordance with Figures 2 and 3, the sequence Cr > Zr > Al > Fe > Ti: that is, Cr-PILC has the highest enhancement in the sorption potential and Ti-PILC the lowest. Thus, if we ignore (temporarily) the molecular sieving properties of PILCs, the adsorption isotherms should indicate that Cr-PILC possesses the highest sorption capacity and Ti-PILC the lowest. Now if we introduce the molecular sieving effect and the physicochemical properties of the adsorbates (dipole moment, quadrupole moment, and polarizability), then the sorption capacities of the various adsorbates on the PILCs change drastically. For instance, Figure 8 shows that the CH_4 sorption capacity on Zr-PILC is higher than that shown for Cr-PILC. The higher CH_4 sorption capacity on Zr-PILC indicates that Cr-PILC contains

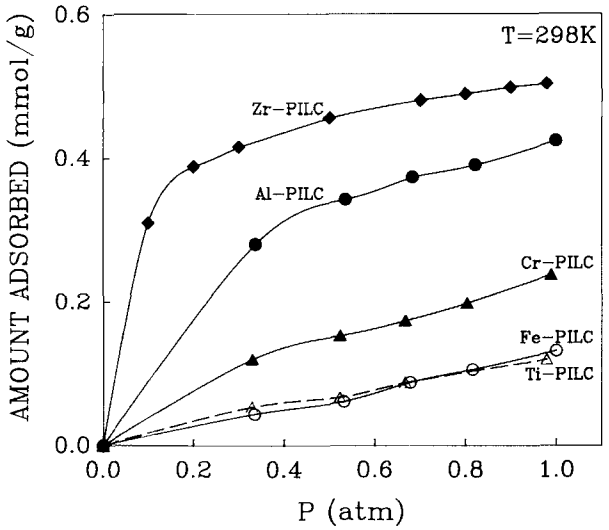

Figure 8. Methane adsorption isotherms at 298 K on Zr, Al, Cr, Fe, and Ti-PILCs.

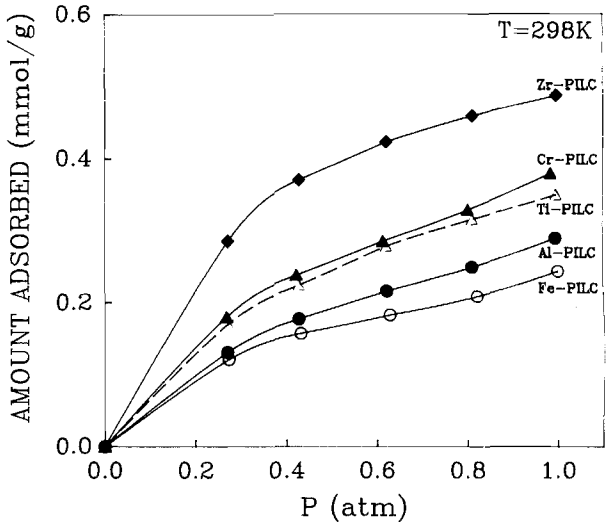

Figure 10. Carbon dioxide adsorption isotherms at 298 K on Zr, Al, Cr, Fe and Ti-PILCs.

a greater fraction of smaller pores (as is evident from Figure 1) that are not accessible to CH_4. In addition, although the enhancement in the sorption potential in Al-PILC is lower than in Cr-PILC, the pores in Al-PILC are large enough to allow CH_4 molecules to penetrate, whereas the narrow pores of Cr-PILC present a greater degree of pore blockage. The pore sizes in Fe and Ti-PILCs are too large, and the enhancement of the sorption potentials are negligible compared to the enhancement in Zr-PILC; consequently, the sorption capacities on Fe and Ti-PILCs are quite small.

Figure 9 shows what happens if we decrease the size of the adsorbate. Note the kinetic diameter of N_2 is smaller than CH_4 (see Table 4). The amount of N_2 adsorbed on Cr-PILC is comparable to the CH_4 sorption capacity shown in Figure 8, indicating that molecular sieving effects are still present. Also, note that the N_2 sorption capacities of Fe and Ti-PILCs are the lowest, due to negligible enhancement in the sorption potentials. The most interesting result in Figure 9 is the remarkable decrease in N_2 sorption capacity on Al-PILC, creating a dramatic increase in the equilibrium selectivity of CH_4/N_2 (compare Figures 8 and 9). However, for Zr-PILC, the N_2 sorption capacity is comparable to the CH_4 sorption capacity shown in Figure 8. A possible explanation for such sorption behaviors lies in the enhancement of adsorption potentials. The N_2 and CH_4 adsorption potentials on Zr-PILC and Al-PILC are shown in Figure 5. Note that the enhancement of the sorption potentials of N_2 and CH_4 on Zr-PILC is comparable, whereas large differences are observed for the sorption potentials in Al-PILC. As the adsorbate size decreases (going from CH_4 to N_2), the adsorbates feel less the influence of the enhancement of the sorption potential for a given pore size. Since Zr-PILC contains much smaller pores than Al-PILC (see Figure 1), a smaller size adsorbate (assuming all other properties remain constant) is required for Zr-PILC to show similar

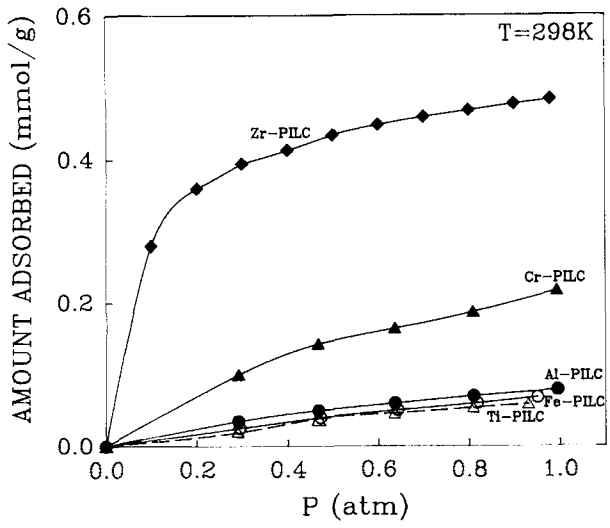

Figure 9. Nitrogen adsorption isotherms at 298 K on Zr, Al, Cr, Fe, and Ti-PILCs.

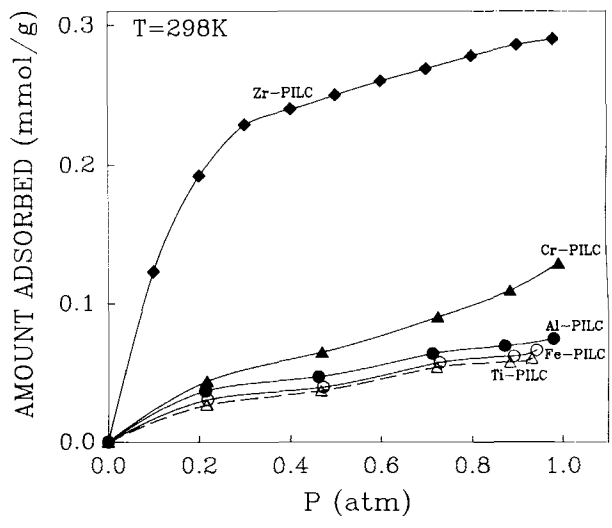

Figure 11. Oxygen adsorption isotherms at 298 K on Zr, Al, Cr, Fe and Ti-PILCs.

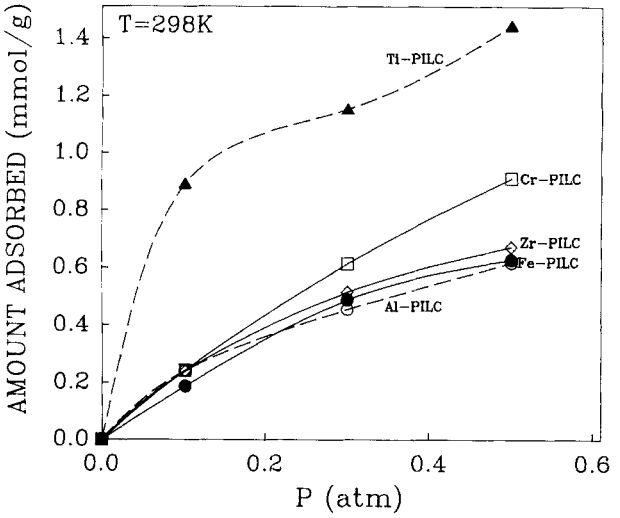

Figure 12. NO adsorption isotherms at 298 K on Zr, Al, Cr, Fe and Ti-PILCs.

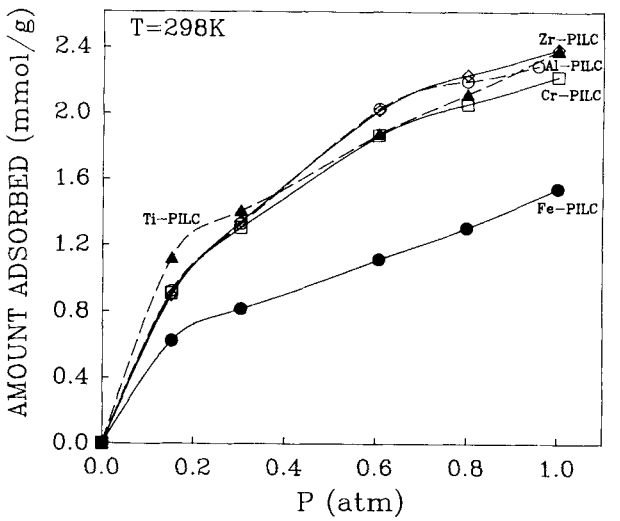

Figure 13. SO_2 adsorption isotherms at 298 K on Zr, Al, Cr, Fe and Ti-PILCs.

sorption behavior displayed by Al-PILC. Thus, N_2 sorption capacity in Zr-PILC is quite high, due to the enhancement of the sorption potential, whereas the N_2 sorption capacity drops, since N_2 molecules experience less influence from the overlapping wall potentials in Al-PILC.

Figure 10 shows that by decreasing further the size of the adsorbate (going from CH_4 to N_2 to CO_2), the molecular sieving effect on Cr-PILC becomes less important, that is, less pore blockage, and the sorption capacity of CO_2 on Cr-PILC becomes more comparable to the sorption capacity of CO_2 on Zr-PILC. Further decrease is anticipated in the size of the adsorbate while fixing other properties (e.g., polarizability, dipole moment, etc.), and the sorption capacity on Cr-PILC will become more comparable and may even exceed Zr-PILC sorption capacity. The O_2 adsorption isotherms are shown in Figure 11. The sorption characteristics follow the same trend as for CO_2 adsorption isotherms given in Figure 10. Although the kinetic diameter of CO_2 is smaller than O_2, the CO_2 adsorption capacities on PILCs are much greater than the O_2 sorption capacities. The reason is O_2 and CO_2 are not quite different in sizes (see Table 4). However, CO_2 possesses large quadrupole moment compared to O_2, as can be seen from Table 4. The permanent quadrupole moment adds considerably to the sorption potential; consequently, CO_2 adsorption is much greater than O_2.

The adsorption isotherms of NO and SO_2 on PILCs are shown in Figures 12 and 13, respectively. The kinetic diameters of SO_2 and NO are almost equal to that of CO_2 (see Table 4). However, the amounts of NO and SO_2 sorbed on these PILCs are much greater than the amount of CO_2 sorbed on the corresponding pillared clay (PILC). The greater NO and SO_2 sorption capacities are due to the permanent dipole moments of these adsorbates (see Table 4). Recall from Figures 6 and 7 that the potential energy profiles obtained using the semi-empirical approach show sizable deviations in comparison to the energy profiles obtained using the Kirkwood-Muller equation that accounts only for the dispersion forces. The large deviations of the energy profiles suggest that Ti-PILC surface has more surface charges than Zr-PILC, therefore, the amount of SO_2 (with permanent dipole moment) sorbed on Ti-PILC becomes comparable to the amount adsorbed on Zr-PILC. Although Zr-PILC has less surface charge, the smaller pores of Zr-PILC provide significant enhancement in the sorption potential. The lower surface area (see Table 3) and surface charge (Figure 7) of Fe-PILC limits the SO_2 sorption capacity and make it less comparable to Ti-PILC and Zr-PILC. The

Table 4. Physical Properties of the Adsorbates*

Sorbate	Size** (nm)	Permanent Dipole Moment (Debye)[†]	Permanent Quad. Moment ($Erg^{1/2}\cdot cm^{5/2}$)	Average Polarizability (cm^3/molecule)	Ionization Potential (eV)[‡]
O_2	0.346	0.0	-0.4×10^{-26}	15.8×10^{-25}	13.62
N_2	0.364	0.0	-1.5×10^{-26}	17.4×10^{-25}	15.58
CH_4	0.380	0.0	—	25.9×10^{-25}	12.6
SO_2	0.360	1.63	—	37.2×10^{-25}	12.34
CO_2	0.330	0.0	-4.3×10^{-26}	29.1×10^{-25}	13.77
NO	0.320	0.167	—	17.0×10^{-25}	9.25

*Values taken from the *CRC Handbook of Chemistry and Physics*, R. C. Weast, M. J. Astle, W. H. Beyer, eds., CRC Press, 67th ed. (1986-1987).
**Values taken from the *Zeolite Molecular Sieves*, D. W. Breck, ed., Wiley-Interscience, New York (1974).
[†]1 debye = 10^{-18} $erg^{1/2}\cdot cm^{3/2}$.
[‡]1 eV = 1.6021×10^{-19} J.

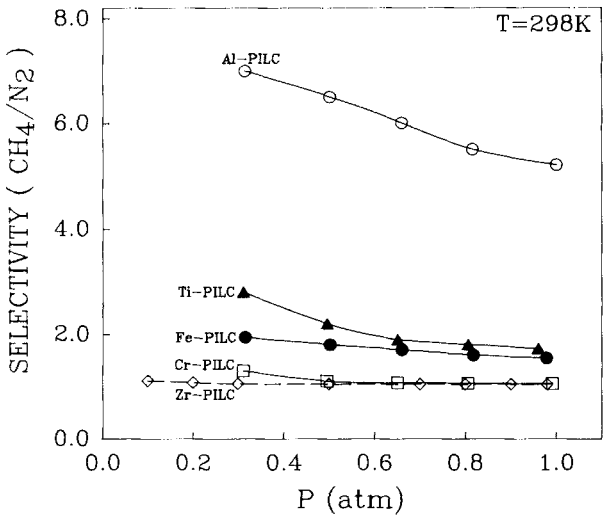

Figure 14. CH_4/N_2 equilibrium selectivities at 298 K on Zr, Al, Cr, Fe and Ti-PILCs.

amount of NO adsorbed on Ti-PILC (see Figure 12) is unexpectedly high compared to that on other PILCs. The reason for this is still unclear, but could be due to the type of pillars present. Thus, in addition to adsorbent's pore sizes and adsorbate's physical properties (such as dipole moment and polarizability), the type of pillars (such as TiO_2, Fe_2O_3, Cr_2O_3, ZrO_2, Al_2O_3) can also affect the sorption characteristics of pillared clays.

A comparison between Figures 12 and 13 indicates that the amount of SO_2 adsorbed on PILCs exceed that of NO adsorbed on these same materials. Since the dipole moment of SO_2 is larger than NO dipole moment, the amount of SO_2 sorbed exceeds that of NO adsorbed. In addition, whenever the adsorbates possess permanent dipole moments and the pores of the adsorbents are large enough to accommodate these adsorbates, the electrostatic forces add to the adsorption potential, that is, the enhancement of the adsorption potential is

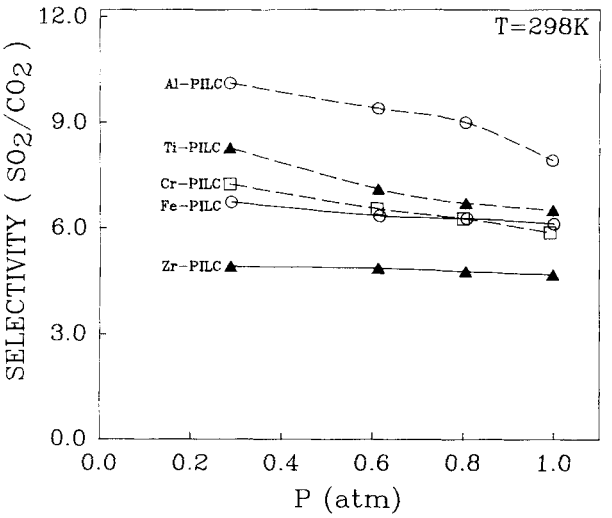

Figure 15. SO_2/CO_2 equilibrium selectivities at 298 K on Zr, Al, Cr, Fe and Ti-PILCs.

increased; consequently, its sorption capacity is greater than the sorption capacity of another adsorbate of similar size (kinetic diameter) and has no dipole moment.

Equilibrium selectivities

The CH_4/N_2 equilibrium selectivities for the five pillared clays are shown in Figure 14. The enhanced CH_4/N_2 selectivity on Al-PILC (≥ 5 at 1.0 atm) is promising indeed for the separation of CH_4 and N_2 as a selectivity for N_2/O_2 about 3.0 on zeolite is adequate for air separation (Yang, 1987). In addition, a selectivity of approximately three appears to be an economic threshold for commercial bulk gas separation application; thus, Al-PILC is a very promising adsorbent for CH_4/N_2 separation.

The SO_2/CO_2 equilibrium selectivities on PILCs are shown in Figure 15. Pressure swing adsorption has recently been considered for the first time (Kikkinides and Yang, 1991) for SO_2/NO_x removal and sulfur recovery from flue gas. The relatively high equilibrium sorption capacities of SO_2 and NO, in addition to the high SO_2/CO_2 selectivities, make pillared clays promising adsorbents for flue gas cleanup applications.

Acknowledgment

This work was supported by the NSF under grant CTS-8914754 and, in part, by the Donors to the Petroleum Research Fund administered by the American Chemical Society. We also thank E. S. Kikkinides for measuring the NO and SO_2 adsorption isotherms.

Notation

A = dispersion constant
a_{mi} = amount adsorbed in the micropores
a^{o}_{mi} = saturated amount adsorbed in the micropores
B = structural parameter in Eq. 9
c = constant in Eq. 10
c = speed of light in Eqs. 3 and 4
d = one-half the distance between the nuclei of two parallel layers in slit-like pore ($d = L/2$)
d_A = diameter of an adsorbate atom
d_a = diameter of an adsorbent atom
d_o = arithmetic mean of diameters of the adsorbate and adsorbent
L = distance between the nuclei of two parallel layers in slit-like pore
m = mass of an electron
n = constant in Eq. 14
N_a = number of atoms per unit area of adsorbent
N_A = number of molecules per unit area of adsorbate
P = pressure
P_o = saturated vapor pressure
q = constant in Eq. 14
r = displacement of an adsorbate molecule from the plane of surface nuclei (one plate)
R = gas constant
T = absolute temperature
W = amount adsorbed
x = half-width of slit-shaped pores, one-half interpillar spacing
x_m = one-half the value of x that corresponds to the maximum in the $G(x)$ distribution
$\bar{x}$ = one-half of the mean pore size
z = distance of adsorbate molecule from the centerline, that is, $z = 0$ corresponds to the adsorbate placed equidistantly between the two plates

Greek letters

α = polarizability
β = affinity coefficient
ϵ = potential energy of interaction in slit-pore

ϵ_{min} = depth of the potential energy well
θ_{mi} = fractional coverage in the micropores
σ = distance from an atom at zero interaction energy
χ = magnetic susceptibility

Subscripts

A = adsorbate
a = adsorbent

Literature Cited

Ackley, M. W., and R. T. Yang, "Kinetic Separation by Pressure Swing Adsorption: Method of Characteristic Model," *AIChE J.*, **36**(8), 1229 (1990).

Adams, D. J., "Grand Canonical Ensemble Monte Carlo for a Lennard-Jones Fluid," *Molec. Phys.*, **29**(1), 307 (1975).

Baes, C. F., and R. E. Mesmer, *The Hydrolysis of Cations*, Wiley, New York (1976).

Baksh, M. S. A., A. Kapoor, and R. T. Yang, "A New Composite Sorbent for Methane-Nitrogen Separation by Adsorption," *Sep. Sci. Technol.*, **25**(7 & 8), 845 (1990).

Baksh, M. S. A., E. S. Kikkinides, and R. T. Yang, "Characterization by Physisorption of a New Class of Microporous Adsorbents: Pillared Clays," *Ind. Eng. Chem.*, in press (1992).

Baksh, M. S. A., and R. T. Yang, "Model for Spherical Cavity Radii and Potential Functions of Sorbates in Zeolites," *AIChE J.*, **37**(6), 923 (1991).

Baksh, M. S. A., "Development, Characterization and Application of New Adsorbents for Separation by Adsorption," PhD Diss., State University of New York, Buffalo (1991).

Bandosz, T., J. Jagiello, and M. Zyla, "Studies of the Chemical Character of Smectite Intercalated with Hydroxy-Alumina," *Chemia Stosowana*, **33**, 189 (1989).

Bartley, G. J. J., and R. Burch, "Zr-Containing Pillared Interlayer Clays: III. Influence of Method of Preparation on the Thermal and Hydrothermal Stability," *Appl. Catal.*, **19**, 175 (1985).

Beutelspacher, H., and H. W. Van Der Marel, "Atlas of Electron Microscopy of Clay and their Admixtures: a Picture Atlas," p. 42, Elsevier Publishing, Amsterdam, London, New York (1968).

Brindley, G. W., and R. E. Sempels, "Preparation and Properties of Some Hydroxy-Aluminum Beidellites," *Clays Clay Miner.*, **12**, 229 (1977).

Burch, R., ed., "Pillared Clays," *Catalysis Today*, Vol. 2, p. 185, Elsevier, New York (1988).

Burch, R., and C. I. Warburton, "Pillared Clays As Demetallisation Catalysts," *Appl. Catal.*, **33**, 395 (1987).

Burch, R., and C. I. Warburton, "Zr-Containing Pillared Interlayer Clays," *J. Catal.*, **97**, 503 (1986).

Carrado, K. A., S. L. Suib, N. D. Skoularikis, and R. W. Coughlin, "Chromium (III)—Doped Pillared Clays (PILCs)," *Inorg. Chem.*, **25**, 4217 (1986).

Derrah, R. I., and D. M. Ruthven, "Sorption of Inert Gases (Ar, Kr, and Xe) in Type A Zeolites," *Can. J. Chem.*, **53**, 996 (1975).

Dubinin, M. M., and H. F. Stoeckli, "Homogeneous and Heterogeneous Micropore Structures in Carboneous Adsorbents," *J. Colloid Inter. Sci.*, **75**, 34 (1980).

Everett, H. D., and J. C. Powl, "Adsorption in Slit-like and Cylindrical Micropores in the Henry's Law Region," *J. Chem. Soc. Farad. Trans. I*, **72**, 619 (1976).

Figueras, F., "Pillared Clays As Catalysts," *Catal. Rev. Sci. Eng.*, **30**, 457 (1988).

Figueras, F., A. Mattrod-Bashi, G. Fetter, A. Thrierr, and J. V. Zanchetta, "Preparation and Thermal Properties of Zr-Intercalated Clays," *J. Catal.*, **119**, 91 (1989).

Hopkins, P. D., B. L. Meyers, and D. M. Van Duch, "Chromium Expanded Smectite Clay," U.S. Patent 4,452,910 (1984).

Horvath, G., and K. Kawazoe, "Method for the Calculation of Effective Pore Size Distribution in Molecular Sieve Carbon," *J. Chem. Eng. Japan*, **16**(6), 470 (1983).

Jaroniec, M., J. Choma, and X. Lu, "An Improved Method for Evaluating the Micropore-Size Distribution from Adsorption Isotherm," *Chem. Eng. Sci.*, **46**(12), 3299 (1991).

Jaroniec, M., and R. Madey, "Gas Adsorption on Structurally Heterogeneous Microporous Solids," *Sep. Sci. Technol.*, **22**(12), 2367 (1987).

Jaroniec, M., and R. Madey, *Physical Adsorption on Heterogeneous Solids*, Elsevier, New York (1988).

June, R. L., A. T. Bell, and D. N. Theodorou, "Prediction of Low Occupancy Sorption of Alkanes in Silicalite," *J. Phys. Chem.*, **94**(4), 1508 (1990).

Kapoor, A., and R. T. Yang, "Kinetic Separation of Methane-Carbon Dioxide Mixture by Adsorption on Molecular Sieve Carbon," *Chem. Eng. Sci.*, **44**, 1723 (1989).

Karavias, F., and A. L. Myers, "Simulation of Single and Binary Gas Adsorption in Zeolite Cavities," *Mol. Simulation*, **8**, 23 (1991).

Kikkinides, E. S., and R. T. Yang, "Simultaneous SO_2/NO_x Removal and SO_2 Recovery from Flue Gas by Pressure Swing Adsorption," *Ind. Eng. Chem.*, **30**, 1981 (1991).

Kiselev, V. A., and P. Q. Du, "Molecular Statistical Calculation of the Thermodynamic Adsorption of Zeolites using the Atom-Atom Approximation," *J. Chem. Soc. Farad. Trans. II*, **77**(1-15), 17 (1981).

Lahav, N., N. Shani, and J. Shabtai, "Cross-Linked Smectites: I. Synthesis and Properties of Hydroxy-Aluminum Montmorillonite," *Clays Clay Miner.*, **26**, 107 (1978).

Lee, W. Y., R. H. Raythatha, and B. J. Tatarchuk, "Pillared-Clay Catalysts Containing Mixed-Metal Complexes: I. Preparation and Characterization," *J. Catal.*, **115**, 159 (1989).

Liche, F. E., D. W. Golightly, and P. J. Lamothe, "Inductively Coupled Plasma-Atomic Emission Spectroscopy," *Methods of Geochemical Analysis*, U.S. Geological Survey Bulletin 1770, U.S. Printing Office (1987).

Metropolis, N., A. W. Rosenbluth, M. N. Rosenbluth, A. H. Teller, and E. Teller, "Equation of State Calculations by Fast Computing Machines," *J. Chem. Phys.*, **21**, 1087 (1953).

Nicholson, D., and N. G. Parsonage, *Computer Simulation and the Statistical Mechanics of Adsorption*, Academic Press, New York (1982).

Occelli, M. L., "Sorption of Normal Paraffins in a Pillared Clay Mineral," *Proc. Int. Cong. Catal.*, **4**, 725 (1984).

Occelli, M. L., "Catalytic Cracking with an Interlayered Clay-A Two-Dimensional Molecular Sieve," *Ind. Eng. Chem. Prod. Res. Dev.*, **22**(4), 553 (1983).

Occelli, M. L., R. A. Innes, F. S. Hwu, and J. W. Hightower, "Sorption and Catalysis on Sodium-Montmorillonite Interlayered with Aluminum Oxide Clusters," *Appl. Catal.*, **14**, 69 (1985).

Occelli, M. L., and R. M. Tindwa, "Physicochemical Properties of Montmorillonite Interlayered with Cationic Oxyaluminum Pillars," *Clays Clay Miner.*, **31**(1), 22 (1983).

Peterson, B. K., K. E. Gubbins, G. S. Heffelfinger, U. M. B. Marconi, and F. Van Swol, "Lennard-Jones Fluids in Cylindrical Pores: Nonlocal Theory and Computer Simulation," *J. Chem. Phys.*, **88**(10), 6487 (1988).

Pinnavaia, T. J., M. S. Tzou, S. D. Landau, and R. H. Raythatha, "On the Pillaring and Delamination of Smectite Clay Catalysts By Polyoxo Cations of Aluminum," *J. Molec. Catal.*, **27**, 195 (1984).

Pinnavaia, T. J., and M. S. Tzou, "Pillared and Delaminated Clays Containing Iron," U.S. Patent 4,665,044 (1987).

Pinnavaia, T. J., M. S. Tzou, and S. D. Landau, "New Chromia Pillared Clay Catalysts," *J. Amer. Chem. Soc.*, **107**, 2783 (1985).

Razmus, D. M., and C. K. Hall, "Prediction of Gas Adsorption in 5A Zeolites Using Monte Carlo Simulation," *AIChE J.*, **37**(5), 769 (1991).

Reid, R. C., and T. K. Sherwood, *The Properties of Gases and Liquids*, 2nd ed., McGraw-Hill, New York (1966).

Rightor, E. G., M. S. Tzou, and T. J. Pinnavaia, "Iron Oxide Pillared Clay with Large Gallery Height: Synthesis and Properties as a Fischer-Tropsch Catalyst," *J. Catal.*, **130**, 29 (1991).

Rowley, L. A., D. Nicholson, and N. G. Parsonage, "Grand Ensemble Monte Carlo Studies of Physical Adsorption I-Results for Multilayer Adsorption of 12:6 Argon in the Field of a Plane Homogeneous Solid," *Molec. Phys.*, **31**, 365 (1976).

Rowley, L. A., D. Nicholson, and N. G. Parsonage, "Grand Ensemble Monte Carlo Studies of Physical Adsorption II-The Structure of the Adsorbate: Critique of Theories of Multilayer Adsorption of 12-6 Argon on a Plane Homogeneous Solid," *Molec. Phys.*, **31**, 389 (1976).

Sahimi, M., T. T. Tsotsis, and M. L. Occelli, "Computer Simulation

of Diffusion, Adsorption and Reaction of Organic Molecules in Pillared Clays," *Mat. Res. Soc. Symp. Proc.*, **111**, 271 (1988).
Saito, A., and H. C. Foley, "Curvature and Parametric Sensitivity in Models for Adsorption in Micropores," *AIChE J.*, **37**(3), 429 (1991).
Shabtai, J., and N. Lahari, "Cross-Linked Montmorillonite Molecular Sieves," U.S. Patent 4,216,188 (1980).
Shabtai, J., F. E. Massoth, M. Tokarz, G. M. Tsai, and J. McCauley, "Characterization and Molecular Shape Selectivity of Cross-Linked Montmorillonite (CLM)," *Proc. Int. Cong. Catal.*, **4**, 735 (1984).
Shabtai, J., M. Rosell, and M. Tokarz, "Cross-Linked Smectites: III. Synthesis and Properties of Hydroxy-Alumina Hectorites and Fluorohectorites," *Clays Clay Miner.*, **32**, 99 (1984).
Soto, J. L., and A. L. Myers, "Monte Carlo Studies of Adsorption in Molecular Sieves," *Molec. Phys.*, **42**(4), 971 (1981).
Sterte, J., "Preparation and Properties of Large-Pore La-Al-Pillared Montmorillonite," *Clays and Clay Miner.*, **39**(2), 167 (1991).
Sterte, J., "Synthesis and Properties of Titaniun Oxide Cross-Linked Montmorillonite," *Clays and Clay Miner.*, **34**(6), 658 (1986).
Stoeckli, H. F., "Microporous Carbons and Their Characterization: the Present State of the Art," *Carbon*, **28**(1), 1 (1990).
Stoeckli, H. F., "A Generalization of the Dubinin-Radushkevich Equation for the Filling of Heterogeneous Micropore Systems," *J. Colloid Int. Sci.*, **59**(1), 184 (1977).
Stroud, H. J. F., E. Richard, P. Limcharoen, and N. G. Parsonage, "Thermodynamic Study of Linde Sieve 5A + Methane System," *J. Chem. Soc. Farad. I*, **72**, 942 (1976).
Suzuki, M., *Adsorption Engineering*, Elsevier, New York (1990).
Suzuki, K., M. Horio, and T. Mori, "Preparation of Aluminum-Pillared Montmorillonite with Desired Pillar Population," *Mat. Res. Bull.*, **23**, 1711 (1988).
Tzou, M. S., and T. J. Pinnavaia, "Chromia Pillared Clays," R. Burch, *loc. cit.*, 243 (1988).
Vaughan, D. E. W., "Multimetallic Pillared Interlayered Clay Products and Processes of Making Them," U.S. Patent 4,666,877 (1987).
Vaughan, D. E. W., R. J. Lussier, and J. S. Magee, "Pillared Interlayered Clay Materials Useful as Catalysts and Sorbents," U.S. Patent 4,176,090 (1979).
Vaughan, D. E. W., R. J. Lussier, and J. S. Magee, "Stabilized Pillared Interlayered Clays," U.S. Patent 4,248,739 (1981).
Warburton, C. I., "Preparation and Catalytic Properties of Iron Oxide and Iron Sulphide Pillared Clays," R. Burch, *loc. cit.*, 271 (1988).
Walker, P. L., Jr., "Chemistry and Physics of Carbon," *A Series of Advances*, Walker, P. L., Jr., ed., Vol. 2, Marcel Dekker, New York (1966).
Woods, B. G., A. Z. Panagiotopoulos, and J. S. Rowlinson, "Adsorption of Fluids in Model Zeolite Cavities," *Molec. Phys.*, **63**(1), 49 (1988).
Yamanaka, S., and G. W. Brindley, "High Surface Area Solids Obtained by Reaction of Montmorillonite with Zirconyl Chloride," *Clays and Clay Miner.*, **27**, 119 (1979).
Yamanaka, S., and G. W. Brindley, "Hydroxy-Nickel Interlayering in Montmorillonite by Titration Method," *Clays and Clay Miner.*, **26**, 21 (1978).
Yamanaka, S., and M. Hattori, "Iron Oxide Pillared Clay," R. Burch, *loc. cit.*, 261 (1988).
Yamanaka, S., T. Doi, S. Sako, and M. Hattori, "High Surface Area Solids Obtained by Intercalation of Iron Oxide Pillars in Montmorillonite," *Mat. Res. Bull.*, **19**, 161 (1984).
Yang, R. T., and M. S. A. Baksh, "Pillared Clays as a New Class of Sorbents for Gas Separation," *AIChE J.*, **37**(5), 679 (1991).
Yang, R. T., *Gas Separation by Adsorption Processes*, Butterworth, Boston (1987).

Manuscript received March 13, 1992, and revision received June 11, 1992.